Multi-Wavelength Variability of the Synchrotron Self-Compton Model for Blazar Emission

Mark W. Sincell

Department of Physics MC 704

The University of Illinois at Urbana-Champaign

1110 W. Green Street

Urbana, IL 61801-3080

Received ______________________; accepted ______________________

ABSTRACT

Motivated by recent reports of strongly correlated radio and X-ray variability in 3C279 (Grandi, etal 1995), we have computed the relative amplitudes of variations in the synchrotron flux at ν and the self-Compton X-ray flux at 1 keV ($R(\nu)$) for a homogeneous sphere of relativistic electrons orbiting in a tangled magnetic field. We consider three cases: the Thomson depth of the sphere (τ_T) varies at fixed magnetic field strength (B), B varies at fixed τ_T and equal fractional changes in τ_T and B. Relative to synchrotron self-Compton scattering without induced Compton scattering, stimulated scattering reduces the amplitude of $R(\nu)$ by as much as an order of magnitude when $\tau_T \gtrsim 1$. When τ_T varies in a fixed magnetic field, R_τ increases monotonically from 0.01 at ν_o, the self-absorption turnover frequency, to 0.5 at $100\nu_o$. Variations in B increase R at all ν, up to a factor of 2 if τ_T is constant, and introduce local extrema in R.

The relative amplitudes of the correlated fluctuations in the radio-mm and X-ray fluxes from 3C279 are consistent with the synchrotron self-Compton model if τ_T varies in a fixed magnetic field and induced Compton scattering is the dominant source of radio opacity. The variation amplitudes are are too small to be produced by the passage of a shock through the synchrotron emission region unless the magnetic field is perpendicular to the shock front.

1. Introduction

Blazars are variable, polarized, flat spectrum extragalactic radio sources with a non-thermal continuum extending to γ-ray energies (*e.g.,* Urry & Padovani 1995). The radio emission from blazars is collimated into narrow beams composed of many individual knots and an optically thick core (Kellerman & Pauliny-Töth 1981). In virtually all blazars, the radio knots appear to separate from the core at speeds greater than the speed of light (Urry & Padovani 1995) and this superluminal motion is strong evidence that blazars are relativistic jets of magnetized plasma viewed along the jet axis (Blandford & Königl 1979). Although the jet model also accounts for such diverse blazar properties as the flat radio spectrum (Kellerman & Pauliny-Töth 1981), the short variability time scales at all energies (*e.g.,* Quirrenbach, *et al.* 1991, Maraschi, *et al.* 1992), the small synchrotron self-Compton X-ray fluxes (Marscher 1987, Ghisellini, *et al.* 1992) and the large γ-ray fluxes (Maraschi, *et al.* 1992), the radiative processes which produce the blazar continuum have not been identified. In this paper, we calculate the relative amplitudes of variations in the radio and X-ray fluxes for one of the most popular models of the blazar continuum, synchrotron self-Compton scattering in a relativistic outflow (Jones, O'Dell & Stein 1974, Marscher 1977, Königl 1981, Ghisellini, *et al.* 1985), and we compare the results to observations of correlated variations on the radio and X-ray flux from 3C279 (Grandi, etal 1995: G95).

Blazar spectra are nearly featureless and a large number of models, which make very different assumptions for the relevant radiation processes, agree qualitatively with snapshots of the radio to γ-ray spectrum (Maraschi, *et al.* 1992, Maraschi, *et al.* 1994, Hartmann *et al.* 1996). At low energies, the flat radio spectrum of compact radio cores can be explained by inhomogeneous synchrotron emission (Marscher 1977, Königl 1981, Ghisellini, *et al.* 1985) or by a homogeneous core that is optically thick to induced Compton scattering (Sincell & Krolik 1994: SK94). The situation at high energies is even more complicated. The X-

and γ-ray emission may be synchrotron emission by high energy electrons (Königl 1981, Ghisellini, *et al.* 1985), radiation from a pair cascade (Blandford & Levinson 1995) or low frequency photons which are inverse Compton scattered by relativistic electrons in the jet. In the last case, the source of the low energy photons could be synchrotron radiation from the jet (the synchrotron self-Compton model, Maraschi *et al.* 1992, Maraschi, *et al.* 1994, Bloom & Marscher 1996), UV radiation from a disk (Dermer, Schlickeiser & Mastichiadis 1992), or some diffuse source of radiation surrounding the jet (Sikora, Begelman & Rees 1994, Ghisellini & Madau 1996). We will consider only synchrotron self-Compton scattering in this paper and ignore other sources for the high energy emission.

The synchrotron self-Compton model for the continuum emission assumes that a single population of relativistic electrons radiates synchrotron photons and subsequently scatters a fraction of these to higher energies (Jones, *et al.* 1974). Fluctuations in either the electron density, the magnetic field strength or the Doppler factor of the emission region will affect the synchrotron and self-Compton fluxes instantaneously. Therefore, variations in the low and high energy fluxes which are uncorrelated, or have significant time delays, cannot be the result of synchrotron self-Compton scattering. The relative amplitudes of the variations in the synchrotron and self-Compton fluxes depends upon which physical parameters change. For example, the fractional change in the high energy flux is twice as large as the fractional change in the optically thin synchrotron flux when the electron density varies, whereas they are equal if the magnetic field or the Doppler factor changes (SK94).

The amplitude of the variations in the synchrotron and self-Compton fluxes also depends upon the relativistic electron distribution. The electron spectrum will flatten with increasing radiation intensity because both the synchrotron and inverse Compton cooling rates increase with increasing radiation energy density. However, these cooling processes are both too slow to have any effect upon the electron distribution in the parsec scale jet

(SK94). Therefore, we neglect the evolution of the electron spectrum in the calculations presented in this paper.

SK94 demonstrated that induced Compton scattering can reduce the amplitudes of variations in the synchrotron radiation when the brightness temperature of the source $T_B \lesssim 2 \times 10^{11}$K. The amplitudes of variations in the self-Compton X-ray flux are unaffected by induced Compton scattering because the X-ray flux is dominated by photons scattered from the high-frequency, low T_B, end of the synchrotron spectrum, where the stimulated scattering optical depth is small. Thus, the relative amplitudes of the variations in the synchrotron flux at the self-absorption turnover frequency and the self-Compton flux at 1 keV are reduced from ~ 0.4 to ~ 0.2 when the induced Compton scattering optical depth is large (SK94).

The continuum emission from 3C279, one of the most intensively monitored blazars, varies coherently over its entire spectrum (Maraschi, *et al.* 1992, Maraschi *et al.* 1994, Hartmann, *et al.* 1996). Recently, G95 used historical light curves to show that the radio-mm and 1 keV X-ray fluxes from 3C279 are strongly correlated. The maximum time resolution of the 3C279 light curves was $\sim$ 70d and the absence of any detectable time delay implies that the radio-mm and X-ray fluxes are from physically related regions separated by $\lesssim$ 0.06pc. While this is consistent with the assumptions of the synchrotron self-Compton theory, the relative amplitudes of the radio and X-ray variations are smaller than predicted (Sincell 1996).

In this paper, we extend previous calculations (SK94, Sincell 1996) and compute the relative amplitudes of variations in the synchrotron self-Compton flux as a function of the frequency of the synchrotron emission. We first define the flux variability ratio (§2) and describe how it is calculated. This ratio is computed for three simple types of variations in §3 and the implications for 3C279 are discussed in §4. We conclude in §5.

2. The Flux Variability Ratio

The time variability of the source spectrum is approximated as a sequence of steady state spectra. We have used the code developed in SK94 to compute the steady-state synchrotron spectrum and self-Compton X-ray flux from a homogeneous sphere containing an isotropic power-law distribution of relativistic electrons

$$\frac{\partial n_e}{\partial \gamma} = n_o \gamma^{-p} \tag{1}$$

for $\gamma \geq \sqrt{2}$. We assume $p = 2.5$ in all the simulations and the normalization (n_o) is fixed by the assumed τ_T. This code incorporates synchrotron absorption and emission, inverse Compton scattering and induced Compton scattering by the relativistic electrons. Stimulated scattering becomes the dominant source of radio opacity when $T_B \gtrsim 2 \times 10^{11}$K (SK94) and must be included when calculating the spectra of compact radio sources. Self-absorption reemerges as the dominant opacity source at low frequencies and inverse Compton scattering of synchrotron photons by electrons with $\gamma \lesssim 10$ contributes to the radio flux above the self-absorption turnover.

The flux variability ratio

$$R_m(\tau_T, B, \nu) = \frac{\partial \log S_r(\tau_T, B, \nu)}{\partial \log S_x(\tau_T, B)}|_m, \tag{2}$$

is the ratio of the fractional change in the synchrotron flux at ν (S_r) and the self-Compton X-ray flux (S_x) at 1 keV caused by a fluctuation in the physical parameter m. In this paper we investigate three different variations: the Thomson depth (τ_T) of the source varies at fixed magnetic field strength ($m = \tau$), the magnetic field strength (B) varies at fixed τ_T ($m = B$) and equal fractional changes in τ_T and B ($m = S$). The third case approximates the passage of a strong shock through the plasma, assuming that the field is tangled (*e.g.*, Marscher & Gear 1985). We also assume that τ_T and B are uniform throughout the source. Simple analytic calculations of R_m are possible for synchrotron self-Compton scattering

(SK94), but R_m must be calculated numerically when the induced Compton scattering opacity is large (SK94).

We compute the variability ratio using the approximate formula

$$R_m(\nu) \simeq \frac{S_r(m,\nu) - S_r(m+\Delta m,\nu)}{S_r(m,\nu) + S_r(m+\Delta m,\nu)} \cdot \frac{S_x(m) + S_x(m+\Delta m)}{S_x(m) - S_x(m+\Delta m)}, \tag{3}$$

and the radio spectra and X-ray fluxes from two models with closely spaced values of the parameter m. In this paper we choose $\Delta m/m = 0.1$ but the results are fairly insensitive to Δm, even when $\Delta m/m \gtrsim 1$ (see figures in Sincell 1996).

3. Results

We have calculated R_τ, R_B and R_S for $0.01 \leq \tau_T \leq 3.0$ and a range of B. In figs. 1, 2 and 3 we plot R_m as a function of ν/ν_o, where ν_o is the synchrotron self-absorption turnover frequency. When the effects of induced and inverse Compton scattering on the radio spectrum are neglected, $R_m(\nu/\nu_o)$ is independent of the unperturbed values of τ_T and B. Including Compton scattering in the computation of the radio spectrum introduces a strong dependence upon τ_T but $R_m(\nu/\nu_o)$ remains nearly independent of B because the induced Compton scattering optical depth at ν_o is $\propto T_B \tau_T \propto B^{-1/(p+4)} \tau_T^{(p+5)/(p+4)}$ (SK94). The code was used to verify that R_m changed by less than a few percent when B increased by two orders of magnitude. Therefore, we present R_m for $B = 10^{-5}$G and use the relation (*e.g.,* SK94)

$$\nu_o \propto \left(\frac{\delta}{1+z}\right) B^{(p+2)/(p+4)} \tag{4}$$

to scale R_m to any desired field strength, Doppler boost (δ) or redshift (z).

Although $R_m(\nu/\nu_o)$ is independent of the unperturbed values of τ_T and B when the effects of Compton scattering on the radio spectrum are neglected, it does depend on which parameters vary. At optically thin frequencies, $\nu \gg \nu_o$, $R_\tau \simeq 0.5$, $R_B \simeq 1.0$ and $R_S \simeq 0.7$,

independent of frequency (figs. 1, 2 and 3). These numerical values are in good agreement with the analytic results in SK94.

Synchrotron self-absorption reduces R_m at $\nu \lesssim \nu_o$. This is because any change in the physical parameters which increases the synchrotron emissivity results in a compensating increase in the opacity and decrease in the photospheric depth. Thus, the net flux at optically thick frequencies is less sensitive to changes in the source parameters. The ratio of the self-absorption opacity to the emissivity increases rapidly as ν/ν_o decreases (*e.g.,* SK94) and R_τ approaches zero at $\nu \lesssim \nu_o/2$. Increasing B also increases ν_o (eq. 4) and the increase in the self-absorption opacity at fixed ν overwhelms the increase in the emissivity when $\nu \ll \nu_o$. The resulting decrease in the synchrotron flux at ν appears as negative values of R_B and R_S (figs. 2 and 3). Negative values of R_m correspond to an anti-correlation of the synchrotron and self-Compton fluxes.

Compton scattering changes the frequency dependence of R_m and introduces a dependence on τ_T (figs. 1, 2 and 3). Induced Compton scattering reduces R_τ over more than a decade in frequency when $\tau_T \gtrsim 0.1$ (fig. 1), relative to the synchrotron self-Compton scattering model without stimulated scattering. R_τ at $\nu \simeq \nu_o$ is reduced by almost an order of magnitude when $\tau_T \gtrsim 1$. The stimulated scattering opacity at low frequencies and the contribution of inverse Compton scattered photons at higher frequencies results in a monotonic increase in R_τ from 0.01 at $\nu \lesssim \nu_o$ to 0.5 at $\nu \sim 100\nu_o$ (fig. 1).

Even though synchrotron self-absorption is the dominant source of opacity, stimulated scattering increases the photon occupation numbers at low frequencies. This increases the synchrotron flux at $\nu \ll \nu_o$ and the anti-correlation of the synchrotron and self-Compton fluxes caused by variations in B disappears when $\tau_T \gtrsim 1$.

Variations in the magnetic field strength introduce local extrema into $R_{B,S}$ when the stimulated scattering optical depth is large. The largest contribution to the induced

Compton scattering opacity at $\nu \lesssim \nu_o$ is from electrons with $\gamma_* = \frac{1}{2}\left(\frac{\nu_m}{\nu}\right)^{1/2}$ where $\nu_m \gtrsim \nu_o$ is the peak of the spectrum (SK94). The low energy cutoff $\gamma = \sqrt{2}$ reduces the stimulated scattering opacity at frequencies $\nu_m/8 \lesssim \nu \lesssim 8\nu_m$ because $\gamma_* < \sqrt{2}$ and there are no electrons which couple ν to ν_m. When synchrotron self-absorption is the dominant source of opacity, the optical depth of the plasma decreases with frequency and R increases with frequency. A local maximum in R appears at the frequency where the stimulated scattering opacity is approximately equal to the synchrotron opacity. At higher frequencies, induced Compton scattering limits the variations in the synchrotron flux and reduces R. The local minimum in R occurs at $\nu \sim \nu_m/8$ where the stimulated scattering opacity reaches a maximum.

These local extrema are not as prominent in R_τ because variations in τ_T increase the optical depth at all frequencies. However, the kink in the $\tau_T = 0.1$ curve of R_τ (fig. 1) is also due to this effect.

4. 3C279

G95 used historical light curves of 3C279 to show that variations in the radio-mm and X-ray fluxes are strongly correlated with a time delay of $\lesssim$ 70 days. They also calculated the logarhithmic dispersion, or variability amplitude ($v(\nu)$), of the available measurements and found that $v(\nu)$ increases systematically with frequency. However, these estimates of $v(\nu)$ are uncertain because many emission components contribute to the observed flux at a given frequency (*e.g.,* Unwin, *et al.* 1989). These components may vary independently and the G95 data lacks the spatial resolution necessary to reliably subtract the non-variable background. Long-term monitoring at higher resolution (VLBA) is necessary to remove this source of uncertainty. In the remainder of this paper we will assume that the variable component dominates the observed flux, but it should be remembered that a significant

amount of non-variable flux at ν will reduce $v(\nu)$ below the value expected for the variable component alone.

Both the strong correlation of the radio and X-ray fluxes and the absence of a detectable time delay between variations in the two bands are consistent with the assumptions of the synchrotron self-Compton model for the continuum emission. We used the variability amplitudes calculated by G95 to estimate

$$R \simeq \frac{v(\nu)}{v(1\mathrm{keV})} \tag{5}$$

at four frequencies in the range 14.5GHz $< \nu <$ 230GHz. The estimated R for the epochs 1988-1991.4 and 1991.4-1993.2 are plotted in fig. 4. The model R_τ for $\tau_T = 1.0$, $B = 10^{-3}$G and $\delta = 20$ is displayed on the same figure.

The relative amplitudes of the variations in the radio and X-ray fluxes from 3C279 are consistent with the synchrotron self-Compton model if τ_T varies in a fixed magnetic field and induced Compton scattering is the dominant source of radio opacity. It is immediately apparent from fig. 4 that the magnitudes of both R_B and R_S are too large to fit the observed values of R for 3C279. In addition, neither the local extrema in R or the anti-correlation of the synchrotron and self-Compton fluxes are observed. We also find that the increase in R with frequency is much slower than expected for the synchrotron self-Compton model without induced Compton scattering (fig. 4). However, both the magnitude and the frequency dependence of R are consistent with R_τ when $\tau_T \gtrsim 1$.

This implies that $\tau_T \sim 1$ in the synchrotron self-Compton emission region. The magnetic field strength and Doppler factor cannot be calculated independently (eq. 4), but the values we have assumed ($B = 10^{-3}$G and $\delta = 20$) are consistent with other estimates of the physical parameters for 3C279 (Ghisellini, etal 1985, Maraschi, *et al.* 1992, SK94). Larger magnetic fields require smaller Doppler factors and vice versa.

We can set a lower limit on the electron density using the variability time scale and the requirement $\tau_T \sim 1$. The linear dimension of the emission region $l \lesssim l_{max} = 1.8 \times 10^{17}\delta$cm if the observed flux varies on a time scale of $\lesssim 70$ days. The stimulated scattering optical depth of the plasma will be large enough to reduce the variability amplitudes if the electron density $n_e \gtrsim 8 \times 10^6 \delta^{-1}$ cm^{-3}. The total particle energy density of the distribution in eq. 1 is dominated by the rest mass energy so $U_e \sim n_e m_p c^2 \sim 7\delta^{-1}\left(\frac{m_p}{m_e}\right)$ ergs cm^{-3}, where $m_{p,e}$ are the masses of the positively charged particle and an electron, respectively. The magnetic energy density $U_B \ll U_e$ and the plasma is far from equipartition.

A strong shock passing through the synchrotron emission region amplifies both the electron density and the magnetic field strength if the magnetic field is either tangled or aligned parallel to the shock front (*e.g.,* Marscher & Gear 1985). Our results for 3C279 indicate that the variations in the flux are due to fluctuations in the electron density alone. Thus, we conclude that if the variations are caused by a shock the magnetic field must be aligned perpendicular to the shock front. An alternative possibility is that the observed variations are due to fluctuations in the local electron density caused by a change in the particle injection rate.

5. Conclusions

We have calculated $R_m(\nu)$, the relative amplitude of variations in the synchrotron flux at ν and the self-Compton X-ray flux at 1 keV, for a homogeneous sphere of relativistic electrons orbiting in a tangled magnetic field. The index m refers to the physical quantity which is assumed to vary and in this paper we investigate three cases: variations in τ_T at fixed B, variations in B at fixed τ_T and equal fractional changes in both quantities. The last case approximates the passage of a strong shock through the plasma (*e.g.,* Marscher & Gear 1985). We find R_m to be useful for two reasons. First, the frequency dependence of

R_m is determined by the optical depth of the plasma. Second, R may be estimated directly from observations of correlated radio and X-ray variability (*e.g.,* G95).

If synchrotron self-absorption is the dominant source of opacity, the frequency dependence of R_m is determined by ν_o, the self-absorption turnover frequency, and the physical parameter which is assumed to vary. We find that R_m is constant at all optically thin frequencies ($\nu \gg \nu_o$) and, for our assumed electron distribution (eq. 1), $R_\tau \simeq 0.5$, $R_B \simeq 1.0$ and $R_S \simeq 0.7$. Self-absorption causes all the R_m to drop sharply at $\nu \lesssim \nu_o$ and both $R_{B,S}$ become negative at $\nu \ll \nu_o$.

Induced Compton scattering reduces R_m over more than a decade in frequency, relative to the synchrotron self-Compton model without stimulated scattering, when $\tau_T \gtrsim 0.1$. Increasing τ_T reduces R_τ at frequencies near ν_o and R_τ can be an order of magnitude smaller than the self-absorbed value when $\tau_T \gtrsim 1$. We find that R_τ increases monotonically from low to high frequencies, but a slight change in the stimulated scattering opacity at $\nu \sim \nu_m/8$ causes local extrema in $R_{B,S}$.

Variations in the Thomson depth of a homogeneous source of synchrotron self-Compton radiation reproduces the relative amplitudes of the correlated radio and X-ray flux variations in 3C279 (G95) if $\tau_T \sim 1$ and the emission region is optically thick to induced Compton scattering. Although B and δ cannot be independently constrained (eq. 4), the observed R is consistent with $B \sim 10^{-3}$G and $\delta \sim 20$. If we assume that the maximum linear dimension of the emission region is $l_{max} \sim 0.06\delta$ pc, as implied by the variability time scale, $\tau_T \sim 1$ requires that the electron density be $n_e \gtrsim 8 \times 10^6 \delta^{-1}$ cm^{-3}. In this case, the particle energy density is much larger than the magnetic field energy density.

Variations in the magnetic field strength result in values of R which are larger than observed. If the observed fluctuations are due to the passage of a shock, the magnetic field must be oriented perpendicular to the shock front. Variations in the local particle injection

rate could change the electron density without necessarily changing the field strength.

Finally, it has been argued that stimulated scattering cannot be important in blazars with optically thick spectral indices of $\alpha = -5/2$ (Litchfield, *et al.* 1995). This argument is erroneous because synchrotron self-absorption *always* becomes the dominant source of opacity, and $\alpha = -5/2$, at low enough frequencies (SK94). However, this points out the ambiguities inherent in attempting to determine the radio opacity using spectral measurements alone. Additional multi-wavelength variability studies (*e.g.,* G95) are clearly necessary to determine the relevant radiative processes in blazars.

We thank the referee, Laura Maraschi, for helpful comments and Stephen Hardy for pointing out the error in the kinetic equation. Support for this work was provided by NASA grants NAGW-1583 and NAG 5-2925, and NSF grant AST 93-15133. The simulations were performed at the Pittsburgh Supercomputing Center (grant AST 960002P).

REFERENCES

Blandford, R. D. & A. Königl 1979 Ap. J., 232, 34

Blandford, R. D. & A. Levinson 1995 Ap. J., 441, 79

Bloom, S. D. & A. P. Marscher 1996 Ap. J., 461, 657

Dermer, C. D., R. Schlickeiser & A. Mastichiadis 1992 Ast. Ap., 256, L27

Ghisellini, G., L. Maraschi & A. Treves 1985 Ast. Ap., 146, 204

Ghisellini, G., P. Padovani, A. Celotti & L. Maraschi 1992 Ap. J., 402, 65

Ghisellini, G. & P. Madau, 1996, preprint

Grandi, P., etal 1995 Adv. Sp. Res., 15,(5) 23 (G95)

Hardy, S.J. and Melrose, D.B., Publications of the Astronomical Society of Australia, 1995, 12, 84

Hartman, R. C., *et al.* 1996 Ap. J., 461, 698

Jones, T. W., S. L. O'Dell & W. A. Stein 1974 Ap. J., 188, 353

Kellerman, K. I. & I. I. K. Pauliny-Töth 1981 Ann. Rev. Astr. Ap., 19, 373

Königl, A. 1981 Ap. J., 243, 700

Litchfield, S. J., J. A. Stevens, E. I. Robson & W. K. Gear 1995 M.N.R.A.S., 274, 221

Maraschi, L., G. Ghisellini & A. Celotti 1992 Ap. J., 397, L5

Maraschi, L., *et al.* 1994 Ap. J., 435, L91

Marscher, A. P. 1977 Ap. J., 216, 244

Marscher, A. P. & W. K. Gear 1985 Ap. J., 298, 114

Marscher, A. P. 1987, in Superluminal Radio Sources, ed J. A. Zensus & T. J. Pearson (Cambridge: Cambridge University Press), 280

Quirrenbach, A., *et al.* 1991 Ap. J. (Letters)., 372,L71

Sikora, M., M. C. Begelman & M. J. Rees 1994 Ap. J., 421, 153

Sincell, M. W. & J. H. Krolik 1994 Ap. J., 430, 550 (SK94)

Sincell, M. W. 1996, to appear in the Proceedings of the Workshop on Blazar Variability, Miami, FL, Feb. 4-7, 1996

Urry, C. M. & P. Padovani 1995 Pub. Ast. Soc. Pacific, 107, 803

Unwin, S.C., M.H. Cohen, J.A. Biretta, M.W. Hodges & J.A. Zensus 1989 Ap. J., 340, 117

A. Correction to the Kinetic Equation

There is an error in the SK94 expression for the contribution of induced Compton scattering to the photon kinetic equation. SK94 transformed the Eulerian time derivative of the photon occupation number to the electron rest frame. However, the correct method is to transform the Lagrangean time derivative (see SK94 eq. 15, and Hardy & Melrose 1994). When this mistake is corrected we find that the expression for the mean rate of change in the photon occupation number caused by stimulated scattering reads

$$\begin{aligned}\langle\frac{Dy(\nu)}{Dt}\rangle &= \frac{3}{128\pi^2}(\sigma_T c)y(\nu)\frac{\partial y}{\partial\nu}\int\frac{d\Omega_e}{4\pi}\int d\gamma\left\{\frac{\partial n_e}{\partial\gamma}\right\}\gamma^{-3} \\ &\times\int d\Omega_1'\int d\Omega_2'(1+\beta\mu_1')^{\alpha-1}(1+\beta\mu_2')^{-(\alpha+3)}\left\{1+(\hat{k}_1'\cdot\hat{k}_2')^2\right\}(\hat{k}_1'\cdot\hat{b}'-\hat{k}_2'\cdot\hat{b}')^2 \qquad (A1)\end{aligned}$$

where $D/Dt = \partial/\partial t + \mathbf{\Omega_1}\cdot\nabla$ is the Lagrangean derivative and the other variables are defined in SK94.

This correction results in two small changes in the formulae of SK94. First, equation 6

This manuscript was prepared with the AAS LaTeX macros v4.0.

should read

$$P(\gamma) = \begin{cases} (2\gamma)^{-(2\alpha+5)} \left\{ \frac{1}{(\alpha-1)^2} + \frac{2}{\alpha(\alpha+1)(\alpha-1)} \right\} & \text{when } \alpha < -1; \\ (2\gamma)^{2\alpha-1} \left\{ \frac{1}{(\alpha+1)^2} - \frac{2}{(\alpha+1)(\alpha+2)(\alpha+3)} \right\} & \text{when } \alpha > -1 \end{cases} . \tag{A2}$$

This change does not affect any of the conclusions in SK94. Second, equation 18 should read

$$\left[\frac{Dy(\nu_1)}{D\tilde{t}}\right]|_{ics} = \frac{1}{12\pi} y(\nu_1) \int \frac{d\Omega_e}{4\pi} \int d\Omega_2 \int \frac{d\nu_2}{\nu_1} \gamma_o^{-p} \frac{\beta_o^2 (1 - \hat{k}_1 \cdot \hat{k}_2)}{|D_1 - D_2|} \frac{\partial y(\nu_2)}{\partial \nu_2}. \tag{A3}$$

The change in the term in the kinetic equation results in an increase in the peak synchroton flux (and T_B) of $\lesssim 7\%$, which is negligible.

Figure Captions

Figure 1. Relative variation in the radio flux density for variations in the Thomson depth as a function of the total Thomson depth of the source. The assumed magnetic field strength is $B = 10^{-5}$G. The solid line, labeled $\tau_T \rightarrow 0$, corresponds to synchrotron self-Compton scattering with neither inverse Compton nor induced Compton scattering included.

Figure 2. Relative variation in the radio flux density for variations in the magnetic field as a function of the total Thomson depth of the source. The assumed magnetic field strength is $B = 10^{-5}$G. The solid line, labeled $\tau_T \rightarrow 0$, corresponds to synchrotron self-Compton scattering with neither inverse Compton nor induced Compton scattering included.

Figure 3. Relative variation in the radio flux density for equal amplitude variations in the Thomson depth and magnetic field strength as a function of the total Thomson depth of the source. This is meant to mimic the variations caused by the passage of a shock through the plasma. The solid line, labeled $\tau_T \rightarrow 0$, corresponds to synchrotron self-Compton scattering with neither inverse Compton nor induced Compton scattering included.

Figure 4. Comparison to the variability amplitudes of 3C279 for the epochs 1988-1991.4 (squares) and 1991.4-1993.2 (triangles). The solid line is the predicted amplitude for synchrotron self-Compton scattering and the dashed line includes induced Compton scattering. The magnetic field strength is $B = 10^{-3}$G, the Thomson depth is $\tau_T = 1.0$ and the Doppler factor is $\delta = 20$.

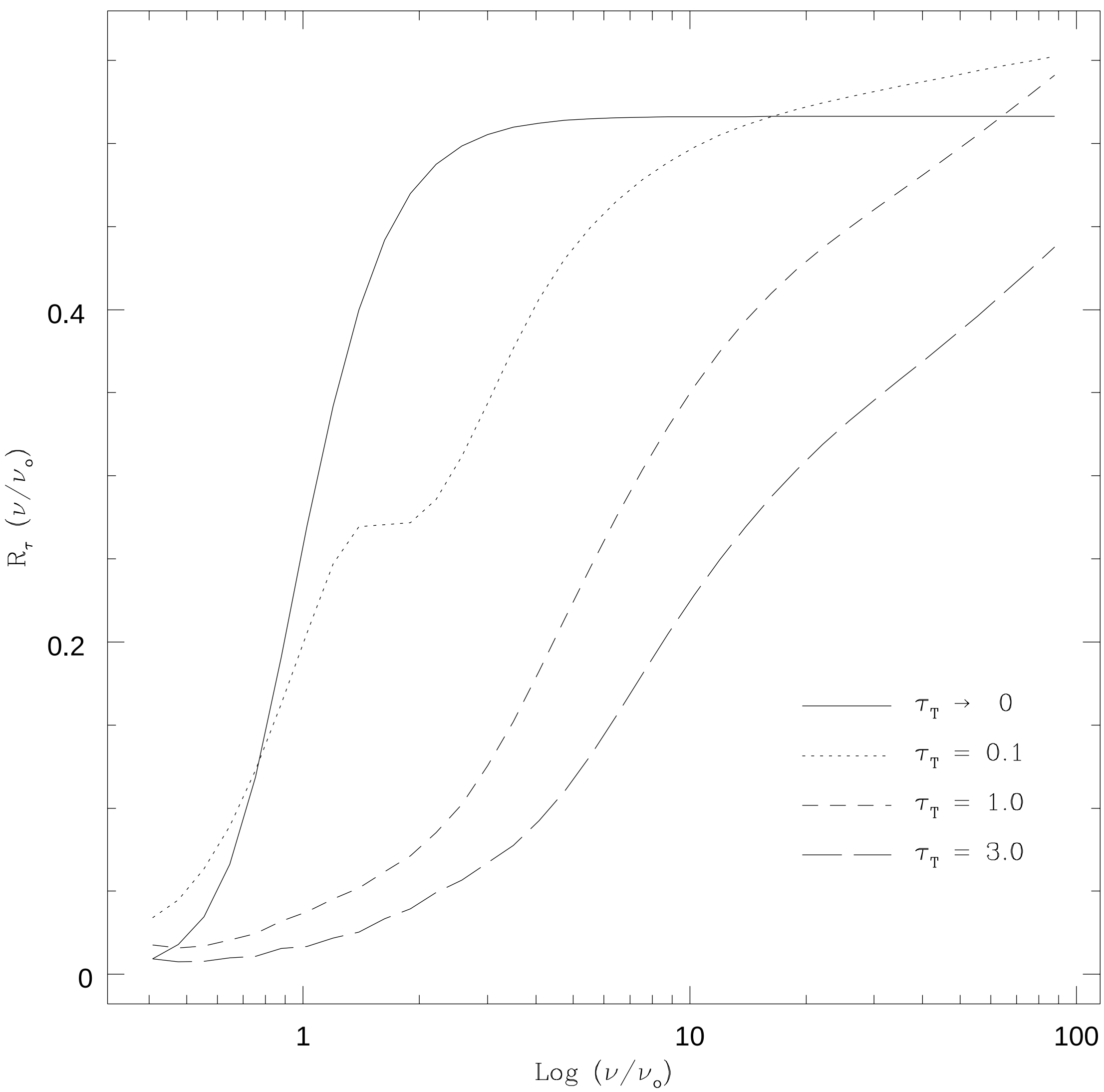
0.4
0.2
0
1
10
100
Log (ν/ν_o)
R_τ (ν/ν_o)
$\tau_T \rightarrow 0$
$\tau_T = 0.1$
$\tau_T = 1.0$
$\tau_T = 3.0$

Fig. 1.—

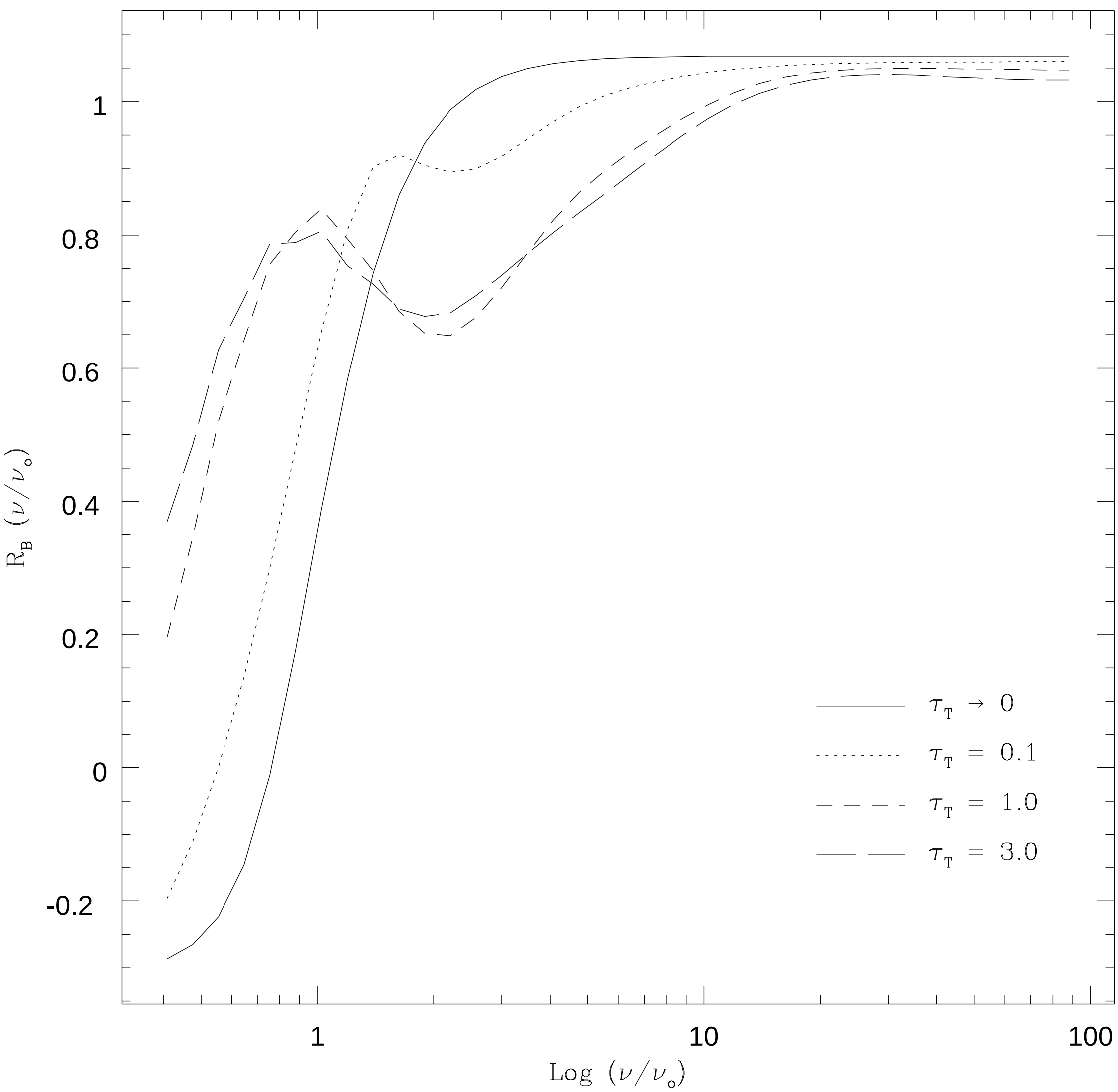

1
0.8
0.6
0.4
0.2
0
-0.2
R_B (ν/ν_o)
1
10
100
Log (ν/ν_o)
$\tau_T \rightarrow 0$
$\tau_T = 0.1$
$\tau_T = 1.0$
$\tau_T = 3.0$

Fig. 2.—

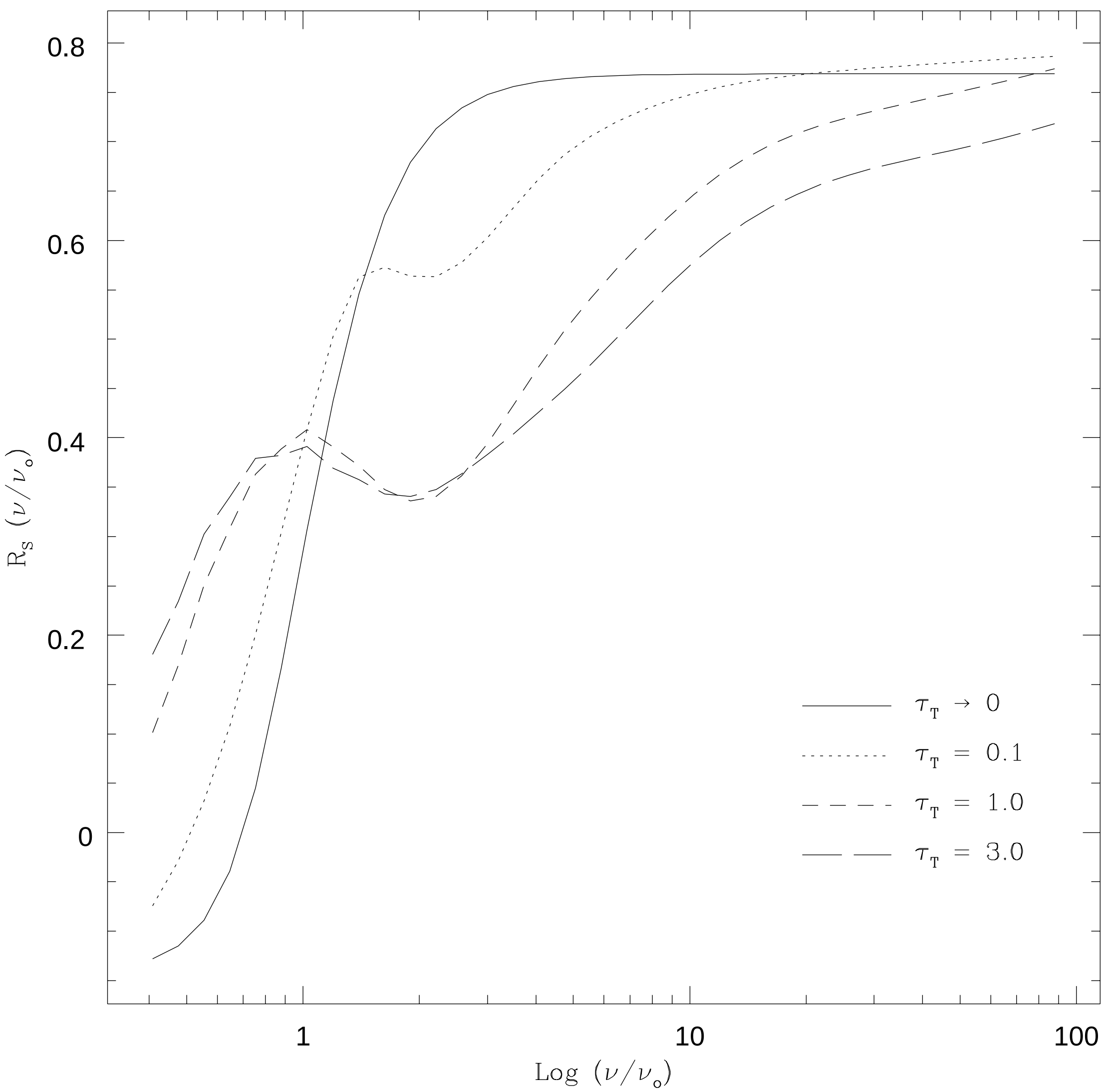
0.8
0.6
0.4
0.2
0
R_S (ν/ν_o)
1
10
100
Log (ν/ν_o)
$\tau_T \to 0$
$\tau_T = 0.1$
$\tau_T = 1.0$
$\tau_T = 3.0$

Fig. 3.—

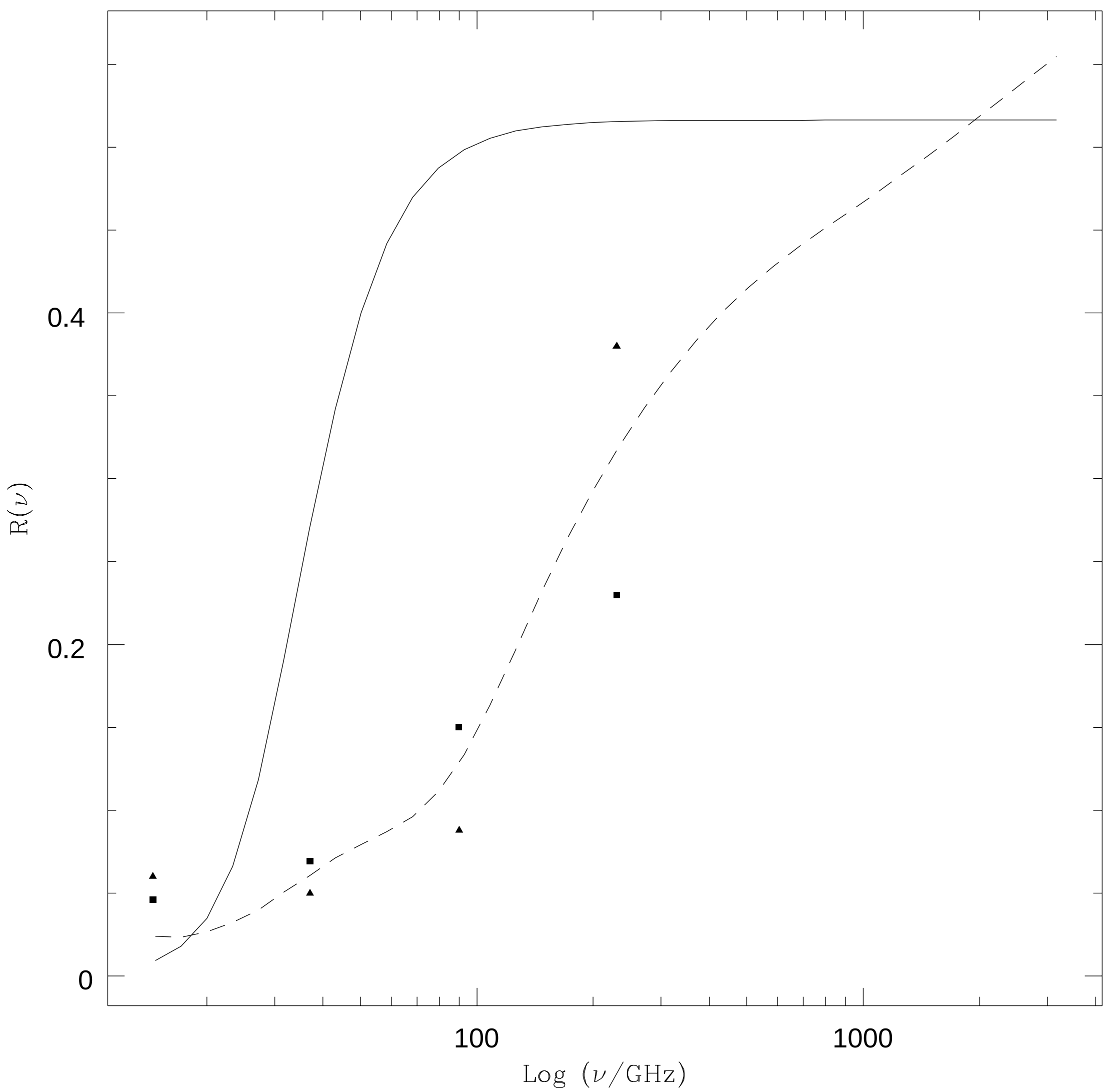

Fig. 4.—